HHS Public Access

Author manuscript

Hum Brain Mapp. Author manuscript; available in PMC 2016 December 01.

Published in final edited form as:

Hum Brain Mapp. 2015 December ; 36(12): 5155–5167. doi:10.1002/hbm.23000.

Coding complexity in the human motor circuit

Elizabeth Heinrichs-Graham[a,b] and **Tony W. Wilson, CA**[a,b,c]

[a]Department of Pharmacology and Experimental Neuroscience, University of Nebraska Medical Center (UNMC), Omaha, NE, USA

[b]Center for Magnetoencephalography, UNMC, Omaha, NE, USA

[c]Department of Neurological Sciences, UNMC, Omaha, NE, USA

Abstract

Cortical oscillatory dynamics are known to be critical for human movement, although their functional significance remains unclear. In particular, there is a strong beta (15-30 Hz) desynchronization that begins before movement onset and continues during movement, before rebounding after movement termination. Several studies have connected this response to motor planning and/or movement selection operations, but to date such studies have examined only the early aspects of the response (i.e., before movement) and a limited number of parameters. In this study, we used magnetoencephalography (MEG) and a novel motor sequence paradigm to probe how motor plan complexity modulates peri-movement beta oscillations, and connectivity within activated circuits. We also examined the dynamics by imaging beta activity before and during movement execution and extracting virtual sensors from key regions. We found stronger beta desynchronization during complex relative to simple sequences in the right parietal and left dorsolateral prefrontal cortex (DLPFC) during movement execution. There was also an increase in functional connectivity between the left DLPFC and right parietal shortly after movement onset during complex but not simple sequences, which produced a significant conditional effect (i.e., complex > simple) that was not attributable to differences in response amplitude. This study is the first to demonstrate that complexity modulates the dynamics of the peri-movement beta ERD, which provides crucial new data on the functional role of this well-known oscillatory motor response. These data further suggest that execution of complex motor behavior may recruit key regions of the fronto-parietal network, in addition to traditional sensorimotor regions.

Keywords

movement; magnetoencephalography; MEG; DLPFC; parietal; beta; oscillations

1. Introduction

In humans, simple, transient movements (real or imagined) are associated with a well-known pattern of oscillatory neural responses in the sensorimotor cortices (Cheyne et al.,

Corresponding Author: Tony W. Wilson, Ph.D., Center for Magnetoencephalography, University of Nebraska Medical Center, 988422 Nebraska Medical Center, Omaha, NE 68198-8422, Phone: (402) 552-6431, Fax: (402) 559-5747, Tony.W.Wilson@gmail.com.

2006, 2008; Gaetz et al., 2010, 2011; Heinrichs-Graham et al., 2014b; Jurkiewicz et al., 2006; Muthukumaraswamy, 2010; Pfurtscheller and Lopes da Silva 1997, Pfurtscheller et al. 1999; Salenius et al. 1997; Schnitzler et al. 1997; Tzagarakis et al., 2010; Wilson et al., 2010, 2011, 2014a). Prior to movement onset there is a strong event-related desynchronization (ERD) in the beta band (15-30 Hz) that starts 0.6-0.8 s before movement, and continues approximately 0.4 s after movement (Cheyne et al., 2006; Engel and Fries, 2010; Gaetz et al., 2010; Heinrichs-Graham et al., 2014b; Jurkiewicz et al., 2006; Wilson et al., 2013; Wilson et al., 2014a; 2010; 2011). This neural response has been reliably localized to regions that include the precentral and postcentral gyri, supplementary motor area, premotor areas, cerebellum, and posterior parietal areas, with many studies reporting activity in several of these regions simultaneously (Cheyne et al., 2006; Gaetz and Cheyne, 2006; Gaetz et al., 2010; Jurkiewicz et al., 2006; Wilson et al., 2014a; 2010). Furthermore, along the precentral and postcentral gyri, this response generally follows the known somatotopic organization of these cortices (i.e., mototopy/somatotopy). Studies have also shown the primary and extended motor regions to be functionally connected (i.e., coherent) in a dynamic way during both continuous movement and rest (Gross et al., 2005; Heinrichs-Graham et al., 2014a; O'Neill et al., 2015; Pollok et al., 2008; Pollok et al., 2006; Pollok et al., 2009; Schoffelen et al., 2008), which suggests that movement execution is served by a broad, coherent sensorimotor network.

While the beta ERD has been recognized as important to movement, only recently have studies begun to characterize its unique functional role. Tzagarakis et al. (2010) used magnetoencephalography (MEG) and a joystick-movement task that involved differing degrees of uncertainty in movement direction. In their task, a variable number of cues, reflecting possible movement directions, were presented prior to the signal to move. They found that the beta ERD during the planning period was inversely related to the number of possible movement directions; that is, with fewer directional cues, indicating greater directional certainty, the amplitude of the pre-movement beta ERD was higher (Tzagarakis et al., 2010). Similarly, Kaiser and colleagues (2001) evaluated the effects of direct and ambiguous cues on the beta ERD during the planning period. They found that on the direct cue trials, beta ERD began significantly earlier, which again suggests that this response was modulated by the certainty of the motor plan (Kaiser et al., 2001). Likewise, Doyle et al. (2005) found that the pre-movement beta ERD was strongly lateralized when movement was cued to one side with certainty, and generally bilateral when the cue gave no directional information. In a related study, Grent-'t-Jong et al. (2014) investigated whether the beta ERD response varied as a function of target separation using MEG. They found that when potential movement directions were more dissimilar, the amplitude of the pre-movement beta ERD was lower than if the potential movement directions were highly similar (Grent-'t-Jong et al., 2014). Taken together, these studies indicate that the beta ERD is strongly associated with the selection and certainty of the pending movement, and thus support the hypothesis that the beta ERD is a movement selection response.

While there is plenty of evidence connecting the beta ERD to movement planning and selection, much less is known about the inherent dynamics of beta ERD activity. It is intuitive that this response plays an important role in movement execution; it begins before movement, is sustained at near peak amplitude during movement, and only dissipates after

movement termination. Of the few studies that have examined the beta ERD during movement execution, all have grouped the planning and execution periods together (e.g., Gaetz et al. 2010; Hall et al. 2011; Wilson et al. 2014; Heinrichs-Graham et al. 2014b) and focused on very simple movements such as single finger taps. Thus, while these studies have identified important characteristics of beta oscillatory activity, they have not been able to address the dynamics and consequently little is known about potential functional differences between pre-movement beta ERD and that occurring later (i.e., after movement onset). Likewise, how the inherent complexity of the movement modulates the beta ERD amplitude and dynamics is also not understood. Given the tight link between pre-movement beta ERD and movement selection, "programming" motor plans that include more complex movements should also result in stronger beta ERD in neural areas serving motor control, although it is unclear whether this process would occur during the planning or execution stages. One aspect that is relatively clear is that complex movements involve regions outside the traditional sensorimotor network. For example, prior invasive studies have implicated the prefrontal cortices and other brain regions serving executive function as important to complex movement selection, especially in the context of sequential movements (Averbeck et al., 2002; 2003; 2006). Furthermore, using local field potentials and a visuomotor task, Zhang et al. (2008) found that pre-movement beta ERD activity in the prefrontal cortex was correlated with reaction time, which provides a link between prefrontal beta and movement execution in macaques.

In the current study, we used a novel motor sequencing paradigm to study the effects of motor plan complexity on peri-movement cortical beta oscillations. The goal of this study was two-fold. First, we sought to identify the inherent dynamics of the beta ERD response by probing neural responses during the planning and movement execution stages separately, and extracting the time series of brain regions exhibiting significant responses. Extracting these time series also enabled us to compute functional connectivity among the involved regions. Secondly, we examined how movement complexity modulated beta ERD activity across the motor network. To this end, high-density MEG was utilized to record participants while they performed sequences of finger movements that varied in complexity. Beta ERD responses during movement planning and execution were independently imaged using beamforming, and the effects of movement complexity on beta ERD amplitude and connectivity were assessed. We hypothesized that an extended network of motor and association cortices would exhibit a strong beta ERD prior to and during movement, and that the amplitude of this response in several brain regions would scale with the inherent complexity of the movement sequence, thereby connecting another critical aspect of motor planning operations to the oscillatory beta ERD response.

2. Methods

2.1 Subject Selection

We studied 19 healthy, right-handed males (mean age: 26.00, range 19-30), all of whom were recruited from the local community. Exclusionary criteria included any medical illness affecting CNS function, neurological or psychiatric disorder, history of head trauma, current substance abuse, and the MEG Laboratory's standard exclusion criteria (e.g., dental braces,

metal implants, battery operated implants, and/or any type of ferromagnetic implanted material). After complete description of the study was given to participants, written informed consent was obtained following the guidelines of the University of Nebraska Medical Center's Institutional Review Board, which approved the study protocol.

2.2 Experimental Paradigm and Stimuli

During MEG recording, participants were seated in a nonmagnetic chair within the magnetically-shielded room. Each participant rested their right hand on a custom-made five-finger button pad (see Figure 1b) while fixating on a crosshair presented centrally. This response pad was connected such that each button sent a unique signal (i.e., TTL pulse/trigger code) to the MEG system acquisition computer, and thus behavioral responses were temporally synced with the MEG data. This allowed accuracy, reaction times, and movement durations (in ms) to be computed offline. In order to create a sufficient baseline, participants initially fixated on a crosshair for 3.75 s before the beginning of each trial (Figure 1a). After this baseline period, a series of three numbers, each corresponding to a finger on the hand (Figure 1b), was presented on the screen in black for 0.5 s. After 0.5 s, the numbers changed color, signaling the participant to tap the fingers corresponding to the motor plan sequentially. The participant was given 2.25 s to complete the motor plan and return to rest. Then, the numbers disappeared and only the fixation crosshair remained. This series of slides constituted one trial; Figure 1a depicts the total time course of a single trial.

There were two conditions corresponding to the complexity of the motor plan. In the "simple" condition, the series of numbers in the plan were sequential (i.e., "1-2-3", "2-3-4", "4-3-2" or "3-2-1"), and thus corresponded to tapping three adjacent fingers. In the "complex" condition, each number in the sequence was at least one number away from the previous number (i.e., "1-4-2", "2-4-1", "3-1-4", or "4-1-3"), and thus mapped to a sequence in which the finger being tapped was not adjacent to the previous finger tapped. Trials were pseudo-randomized, and sequences were controlled for several different variables. First, across conditions we controlled for the first finger tapped, ensuring that any delays related to the ease at which a specific button could be pressed were even between conditions, and thus could not skew reaction time data. Secondly, the sequences in each condition contained the same amount of total movement (i.e., three finger taps) and the same fingers tapped, ensuring that the same neuronal populations were active in each condition and ultimately programmed the same number of movements. A total of 80 trials per condition were completed (160 total trials), making overall MEG recording time about 16 minutes for the task.

2.3 MEG Data Acquisition

All recordings were conducted in a one-layer magnetically-shielded room with active shielding engaged. Neuromagnetic responses were sampled continuously at 1 kHz with an acquisition bandwidth of 0.1–330 Hz using an Elekta MEG system with 306 magnetic sensors (Elekta, Helsinki, Finland). Using MaxFilter (v2.2; Elekta), MEG data from each subject were individually corrected for head motion and subjected to noise reduction using the signal space separation method with a temporal extension (Taulu and Simola, 2006; Taulu et al., 2005).

2.4 MEG Coregistration & Structural MRI Processing

Prior to MEG measurement, four coils were attached to the subject's head and localized, together with the three fiducial points and scalp surface, with a 3-D digitizer (Fastrak 3SF0002, Polhemus Navigator Sciences, Colchester, VT, USA). Once the subject was positioned for MEG recording, an electric current with a unique frequency label (e.g., 322 Hz) was fed to each of the coils. This induced a measurable magnetic field and allowed each coil to be localized in reference to the sensors throughout the recording session. Since coil locations were also known in head coordinates, all MEG measurements could be transformed into a common coordinate system. With this coordinate system, each participant's MEG data were coregistered with structural T1-weighted MRI data prior to source space analyses using BESA MRI (Version 2.0). Structural MRI data were aligned parallel to the anterior and posterior commissures and transformed into the Talairach coordinate system (Talairach and Tournoux, 1988). Following beamformer analysis, each subject's functional images were transformed into standardized space using the transform applied to the structural MRI volume and spatially resampled.

2.5 MEG Time-Frequency Transformation and Statistics

Cardio-artifacts were removed from the data using signal-space projection (SSP), which was accounted for during source reconstruction (Uusitalo and Ilmoniemi, 1997). The continuous magnetic time series was divided into epochs of 5.8 s duration, with 0.0 s defined as movement onset (i.e., first button press) and the baseline defined as the −2.3 to −1.6 s time window (i.e., before movement onset; Figure 1a). Epochs containing artifacts were rejected based on a fixed threshold method, supplemented with visual inspection. After artifact rejection, an average of 65.8 (SD: 5.2) epochs in the simple and 66.8 (SD: 3.2) epochs in the complex condition remained; this difference was not significant, $t(16) = 0.905$, $p = .38$.

Artifact-free epochs were transformed into the time-frequency domain using complex demodulation (resolution: 2.0 Hz, 25 ms; (Papp and Ktonas, 1977)) and the resulting spectral power estimations per sensor were averaged over trials to generate time-frequency plots of mean spectral density. These sensor-level data were normalized by dividing the power value of each time-frequency bin by the respective bin's baseline power, which was calculated as the mean power during the −2.3 to −1.6 s time period. The specific time-frequency windows used for imaging were determined by statistical analysis of the sensor-level spectrograms across the entire array of gradiometers. Each data point in the spectrogram was initially evaluated using a mass univariate approach based on the general linear model. To reduce the risk of false positive results while maintaining reasonable sensitivity, a two stage procedure was followed to control for Type 1 error. In the first stage, one-sample t-tests were conducted on each data point and the output spectrogram of t-values was thresholded at $p < 0.05$ to define time-frequency bins containing potentially significant oscillatory deviations across all participants and conditions. In stage two, time-frequency bins that survived the threshold were clustered with temporally and/or spectrally neighboring bins that were also above the ($p < 0.05$) threshold, and a cluster value was derived by summing all of the t-values of all data points in the cluster. Nonparametric permutation testing was then used to derive a distribution of cluster-values and the significance level of the observed clusters (from stage one) were tested directly using this

distribution (Ernst, 2004; Maris and Oostenveld, 2007). For each comparison, at least 10,000 permutations were computed to build a distribution of cluster values. Based on these analyses, time-frequency windows that corresponded to events of a priori interest (i.e., the peri-movement beta ERD) and contained a significant oscillatory event across all participants and conditions were subjected to the beamforming analysis. Further information is provided in the Results.

2.6 MEG Imaging & Statistics

Cortical networks were imaged through an extension of the linearly constrained minimum variance vector beamformer (Van Veen et al., 1997), which employs spatial filters in the frequency domain to calculate source power for the entire brain volume. The single images are derived from the cross spectral densities of all combinations of MEG gradiometers averaged over the time-frequency range of interest, and the solution of the forward problem for each location on a grid specified by input voxel space. Following convention, the source power in these images was normalized per participant using a separately averaged pre-stimulus noise period of equal duration and bandwidth (Van Veen et al., 1997). MEG pre-processing and imaging used the Brain Electrical Source Analysis (BESA version 6.0) software.

Normalized source power was computed for the selected time-frequency bands over the entire brain volume per participant at 4.0 × 4.0 × 4.0 mm resolution. The effect of sequence condition (“simple” vs. “complex”) was examined using a random effects analysis for the time-frequency bins of interest. Paired-sample t-tests were conducted to probe differences in peri-movement beta ERD as a function of complexity. As with the sensor-level analysis, a two-stage approach was used to control for Type 1 error. In the first stage, t-tests were conducted on each voxel and the output was thresholded at ($p < 0.05$) to create statistical parametric maps (SPMs) showing clusters of potentially significant activation. A cluster value was derived in stage two, for each cluster surviving stage one, by summing all of the t-values of all data points (voxels) within the cluster. Subsequently, permutation testing was used to derive a distribution of cluster-values, and the observed clusters were tested for significance using this distribution (Ernst, 2004; Maris and Oostenveld, 2007). For each comparison at least 1,000 permutations were computed to build a distribution of cluster values.

2.7 Peak Voxel Extraction and Analysis

Following statistical analysis of the beamformer images, we extracted virtual sensors corresponding to the peak voxel per **cluster** for the **significant** task and conditional effects. Briefly, we identified the peak voxel of each task effect by conducting a one-sample t-test across both conditions. This t-test yielded a SPM and we selected the voxel with the highest t-value per significant cluster for virtual sensor extraction. To create the virtual sensors, we applied the sensor weighting matrix derived through the forward computation to the preprocessed signal vector, which yielded a time series for the specific coordinate in source space. Note that this virtual sensor extraction was done per participant and condition individually, once the coordinates of interest (i.e., one per cluster) were known. The same procedure was followed for the virtual sensors corresponding to conditional effects, except

that the peak coordinates per significant cluster were derived from a SPM that was computed using a paired-samples t-test (i.e., complex compared to simple). The virtual sensors corresponding to the peak task effects (i.e., one-sample t-test across both conditions) were used to evaluate the time course of neuronal activity in brain regions where significant oscillatory responses were detected, and phase coherence was used to examine functional connectivity across the network where conditional effects emerged (i.e., complex > simple).

To compute phase coherence, we extracted the phase-locking value (PLV) using the method described by Lachaux et al. (1999). The virtual sensor signals were band-pass filtered at ±2.0 Hz, and their convolution was computed using a complex Gabor wavelet centered at the target frequency. We extracted the phase of the convolution for each time-frequency bin per trial, and then evaluated the phase relationships amongst pairs of brain regions across trials to derive the PLV for the specific pair of regions. The PLV reflects the intertrial variability of the phase relationship between pairs of brain regions as a function of time. Values close to 1 indicate strong synchronicity (i.e. phase-locking) between the two voxel time series' within the specific time-frequency bin across trials, whereas values close to 0 indicate substantial phase variation between the two signals, and thus, low synchronicity (connectivity) between the two regions across trials. To examine connectivity differences between simple and complex movement conditions, the phase coherence spectrograms were examined using paired-samples t-tests for each pair of brain regions across time, and was subjected to the same two-stage statistical testing approach as was used with the sensor- and source-level analyses to control for Type 1 error.

3. Results

3.1 Behavioral Results

All participants were able to successfully complete the task. Two participants were excluded from all statistical analyses due to excessive artifacts in their MEG data. Participants performed well, with an average accuracy of 96.61% (SD: 3.29%) in the simple condition and 97.21% (SD: 2.86%) in the complex condition. Reaction times (i.e., first button press) for the simple and complex conditions were 479.92 ms (SD: 109.63 ms) and 533.95 ms (SD: 103.53 ms), respectively. While differences in accuracy were not significant, $t(16) = 0.940$, $p = 0.361$, differences in reaction time between conditions was statistically significant, $t(16) = 5.45$, $p < .0001$. Finally, movement duration (i.e., how long it took to complete the tapping sequence) was significantly different between conditions, $t(16) = 4.27$, $p < .0001$. Mean movement duration for the simple and complex conditions were 566.17 (SD: 201.49) ms and 630.57 (SD: 194.58) ms, respectively. Behavioral results are shown in Figure 2. To control for these behavioral differences across conditions, we synced our MEG data analyses with movement onset in each trial and focused all analyses on the time windows preceding and during the early stages of movement execution (i.e., before movement termination in either condition).

3.2 MEG Sensor-Level Results

Sensor-level time–frequency spectrograms indicated the typical response pattern of pre-movement alpha and beta desynchronizations, followed by a post-movement beta rebound

(PMBR), in all participants. These spectrograms were statistically examined using one sample t-tests of the sensor-level plots from both conditions together to derive the precise time-frequency bins for subsequent beamforming analyses. Significant peri-movement beta ERD was found in a large number of sensors near the sensorimotor cortex in the 16-26 Hz range from about 0.5 s before movement onset until about 0.75 s afterward ($p < .0001$, corrected; Figure 3). There was also a significant beta synchronization (i.e., PMBR) that extended from about 1.0 s to 3.0 s after movement onset ($p < .0001$, corrected), and a significant alpha desynchronization that persisted from about 0.7 s before movement onset until about 1.2 s after (i.e., −0.7 to 1.2 s), consistent with the motor-related alpha response ($p < .0001$, corrected). In order to distinguish differences in beta activity related to movement planning versus movement execution, the significant beta ERD response period was divided into two temporally-distinct 16-26 Hz windows (i.e., motor planning: −0.45 to 0.0 s; motor execution: 0.0 to 0.45 s; 0.0 s defined as movement onset), and these windows were independently imaged in each participant using a baseline period (−2.2 to −1.75 s before movement onset) to determine the precise brain regions generating these significant oscillatory responses.

3.3 Neuroanatomical Results

3.3.1 Beamforming analysis—Analysis of both simple and complex movements indicated significant beta ERD task effects in the bilateral primary motor cortices (stronger in the contralateral), superior parietal regions, cerebellum, and the supplementary motor area (SMA) during both the movement planning and execution time windows (both p's < .0001, corrected; Figure 4). To more precisely examine the dynamics, we extracted virtual sensors from the peak voxel in each region, which further confirmed the temporal progression and strength of neuronal activity that was discernable in the discrete beamformer images of each condition (see Figure 4).

Statistical analysis of conditional effects using paired-samples t-tests showed that, during movement execution (0.0 to 0.45 s, 16-26 Hz), beta ERD responses were stronger in the left dorsolateral prefrontal cortex (DLPFC; $p < .001$, corrected) and the right superior parietal cortices ($p < .001$, corrected) during complex compared to simple movement sequences (see Figure 5). Interestingly, oscillatory neural responses did not differ between simple and complex movements during the planning phase (−0.45 to 0.0 s, 16-26 Hz) in any brain region. Although the beta ERD was the focus of our study, we anecdotally observed an increase in the PMBR during complex compared to simple movements in the time series of a small number of brain regions (e.g., the left precentral gyrus time series; see Figure 4). Briefly, across both conditions, this response followed the typical trajectory of the well-studied PMBR response, which has been shown to last at least 3.0 s after movement (Cassim et al., 2001; Heinrichs-Graham et al., 2014a; Houdayer et al., 2006; Jurkiewicz et al., 2006; Kurz et al., 2014; Parkes et al., 2006; Wilson et al., 2014a; Wilson et al., 2010; Wilson et al., 2011). However, we did not directly probe this response for several reasons. First, the focus of this study was on how movement complexity modulates the dynamics of the beta ERD response during planning and execution, and the PMBR is a different beta response that occurs after movement have been terminated. Secondly, the PMBR is tightly yoked to the termination of movement and since there were significant differences in movement duration

between our conditions, any potential alteration in the PMBR response would be confounded by performance differences. Thus, any neurophysiological changes in the PMBR would not be interpretable.

3.3.2 Functional connectivity analysis—To examine differences in network-level activity between simple and complex movement sequences, we computed the transient phase-locking values (PLV) between virtual sensors taken from the brain regions where significant beta ERD differences were detected (i.e., left DLPFC and right superior parietal cortex). These analyses indicated a significant increase in beta phase synchrony between the left DLPFC and the right parietal cortices from 0.075 to 0.175 s after movement onset during the complex compared to the simple condition ($p = 0.05$, corrected). Specifically, phase coherence in the two conditions was relatively equal throughout the trial, but there was a sharp, transient increase in phase coherence shortly after movement onset (i.e., 0.075 to 0.175 s) in the complex but not the simple condition. This transient increase in the complex condition was significantly greater than baseline ($p = .017$, corrected; see Figure 6). To ensure these alterations in phase synchrony were not attributable to signal-to-noise differences, we ran a correlation between peak beta ERD amplitude in each brain region and the PLV in both the simple and complex conditions. There were no correlations between the amplitude of activity in the left DLPFC or right partial cortices and the PLV between these regions in either condition (all p's > 0.75); thus, the transient increase in PLV immediately following movement onset was not related to differences in beta ERD amplitude.

4. Discussion

In this study, we used a novel, transient, motor sequence paradigm to study the effects of motor plan complexity on the dynamics of peri-movement cortical beta oscillations in healthy adults. We found that when participants performed each tapping sequence, regardless of complexity, they exhibited strong beta desynchronization in the bilateral primary motor cortices (stronger on the contralateral side), parietal regions, cerebellum, and the SMA. Further, when the motor plan was more complex, participants exhibited a stronger beta ERD in the right parietal cortices and left DLPFC during movement execution, but not during the motor planning stages. Finally, during complex but not simple movement sequences, we observed a sharp transient increase in connectivity between the left DLPFC and right parietal area shortly after movement onset. Below, we discuss the implications of these results for understanding the functional significance of the beta ERD, its dynamics, and how the response is modulated by movement complexity.

We were initially surprised that there were no differences in beta ERD amplitude between the simple and complex conditions during the planning period, nor were there any differences in movement planning or execution in the core sensorimotor regions such as the precentral and postcentral gyri, SMA, and premotor cortices. We suggest that, from a cognitive perspective, movement planning was very similar between conditions in this task (i.e., number of movements, individual movement options), and hence the complex/simple distinction was only illuminated when participants began to carry out the motor plan. Similarly, given the comparable movement plans between conditions, primary movement execution regions such as the precentral gyri are likely to utilize a similar neuronal

population to execute both simple and complex movements, and as such are likely to exhibit a similar population-level motor response (i.e., peri-movement beta ERD) in these regions. Alternatively, it is likely that secondary regions such as the left DLPFC and right parietal cortex were recruited in addition to primary motor areas in order to support the increase in executive planning and coordination required to execute the complex sequences relative to the simple sequences. Likewise, one would also expect the SMA and cerebellum, based on prior literature (e.g., (Ashe et al., 2006; Chan et al., 2006; Glickstein and Doron, 2008; Hoshi and Tanji, 2004; Nachev et al., 2008; Rocca et al., 2009; Stefanescu et al., 2013; Wilson et al., 2014b), to be more strongly recruited for complex sequences, and such a trend was apparent in the virtual sensor and beamformer data of the SMA and cerebellum, but neither region survived multiple comparisons correction.

Our most important finding was likely the significantly increased beta ERD during the execution of complex relative to simple movement sequences in the right parietal cortices and left DLPFC during movement execution. Previous studies using EEG, MEG, invasive recording methods, and functional magnetic resonance imaging (fMRI) have implicated these brain regions in the selection of movement targets and movement planning (Cui and Andersen, 2011; Thoenissen et al., 2002). Recent work recording from parietal cortices in behaving primates, specifically the parietal reach region, showed an increase in neuronal firing during the evaluation of multiple alternative movements, as well as a distinct area that started firing when the movement plan was selected (Cui and Andersen, 2011). Similar results have also been found using fMRI (Thoenissen et al., 2002) and MEG (Park et al., 2013) in humans, suggesting a definitive role of the parietal lobe in movement coordination. Other evidence supporting such a role has emerged from recent studies using transcranial direct-current stimulation (tDCS) and magnetic stimulation (TMS). Specifically, stimulation of the parietal cortices has been shown to modulate motor sequencing abilities and reach planning, and their integration with other motor control centers (Chao et al., 2013; Convento et al., 2014; Krause et al., 2014). For example, Convento and colleagues (2014) stimulated the primary motor and parietal cortices bilaterally and studied the effects on skilled motor function. They found that applying excitatory tDCS to the ipsilateral parietal, as well as the contralateral primary motor cortex, were each associated with improved motor function, whereas inhibitory tDCS to these regions was associated with decreased motor function (Convento et al., 2014).

The left DLPFC is known to be critical for executive functioning operations, including working memory processing and the planning of multi-step movements. Numerous studies using invasive recordings in primates show that the DLPFC is particularly important in performing sequential movements. For example, across a series of non-human primate studies, Averbeck and colleagues (2002; 2003; 2006) found that neurons in the prefrontal cortex fired not only preferentially to the type of movement involved, but also preferentially to the rank-order of movements; that is, certain populations of neurons preferentially fired during performance of the first movement in a sequence, while others preferentially fired for the second or third movement, and so on (Averbeck et al., 2002; 2003). Neurons in this brain area also increased their firing rate as a function of movement certainty (Averbeck et al., 2006), similar to work investigating peri-movement beta oscillatory activity in humans. Thus, the DLPFC is a critical contributor to motor sequencing, and one would expect this

brain area to be differentially activated as a function of movement complexity, which is in line with the current study. In addition, we found a significant difference between the complex and simple conditions in reaction time, which suggests that motor sequence packaging and/or initiation was much more difficult in the complex condition. Moreover, movement duration was significantly different between the two conditions. This pattern of behavioral results suggests a more 'online' motor planning/execution process by which the motor plan for complex movements had to be modified during movement execution, whereas the motor plan in the simple condition was executed without modification. Such additional planning and modifying likely requires a more executive role in performing complicated motor sequences, which helps explain the increase in the DLPFC during complex relative to the simple condition.

Finally, the current results also showed differential patterns of phase coherence (i.e., functional connectivity) between the simple and complex movement conditions. Specifically, phase coherence estimates in each condition were relatively stable and basically equal for most of the time course, but there was a sharp, transient increase in phase locking between the left DLPFC and right parietal cortices that occurred shortly after movement onset during complex, but not simple movement sequences. These results indicate that the execution of more complex movements likely requires a temporary strengthening of connectivity between the left DLPFC and right parietal areas during the early stages of movement execution. Interestingly, several recent MEG studies using dynamic imaging of coherent sources (DICS; (Gross et al., 2001)) have begun to identify task-dependent connectivity patterns within the motor network (Gross et al., 2005; Pollok et al., 2006; 2009). For example, Pollok and colleagues (2008) had healthy participants perform a bimanual finger-tapping task, during which the pace of tapping was either regular or random. They found a coherent motor network consisting of the primary motor cortices, premotor cortex, posterior parietal lobes, cerebellum, and thalamus, and that significant synchrony involving the parietal region occurred during, and not before, movement in the randomly-paced condition (Pollok et al., 2008).

This study was the first to identify the effects of movement complexity on peri-movement cortical beta dynamics. We found that participants exhibited stronger peri-movement beta desynchronization in the left DLPFC and right parietal cortices during the execution of complex relative to simple sequences. In addition, shortly after movement onset, functional connectivity was stronger between the DLPFC and parietal cortices during complex but not simple movements, and this alteration was not attributable to signal strength differences in either brain region. Future studies should utilize neuromodulatory mechanisms such as tDCS or tACS (alternating-current stimulation) in conjunction with MEG to determine the impact of inhibition or excitation of these brain areas on the beta ERD and movement performance. Previous studies using beta-frequency tACS in the primary motor cortex found that, during stimulation (i.e., inhibition of beta ERD), participants moved significantly slower than participants who did not receive stimulation (Pogosyan et al., (2009). In a related study, Joundi and colleagues (2012) used tACS to modulate activity in the motor cortex at the beta as well as the gamma frequency, and found that tACS at the beta frequency slowed movement speed, while tACS at the gamma frequency enhanced movement speed (Joundi et al., 2012). These studies suggest that absolute levels of beta ERD are critical to proper

movement execution, although the dynamics of such effects and the impact of parameters such as complexity remain to be resolved. In conclusion, this study was the first to investigate how movement complexity modulated the spatiotemporal dynamics of peri-movement beta desynchronization. We found that the effects of complexity were most apparent during movement execution, and that more complex sequences elicited stronger beta ERD responses in the left DLPFC and right parietal cortices, as well as stronger functional connectivity within this network. Finally, these results may provide targets outside the "traditional" sensorimotor regions for neuromodulatory therapy (e.g., tDCS) in patients with movement disorders such as Parkinson's disease and cerebral palsy, as previous studies have linked pathological motor-related beta oscillatory activity to these conditions (Heinrichs-Graham et al., 2014a; 2014b; Kurz et al., 2014).

Acknowledgements

This work was supported by NIH grant R01 MH103220 (TWW), the Shoemaker Prize from the University of Nebraska Foundation (TWW), a Kinman-Oldfield Award for Neurodegenerative Research from the University of Nebraska Foundation (TWW), and a grant from the Nebraska Banker's Association (TWW). The Center for Magnetoencephalography at the University of Nebraska Medical Center was founded through an endowment from an anonymous donor. The funders had no role in study design, data collection and analysis, decision to publish, or preparation of the manuscript.

References

Ashe J, Lungu OV, Basford AT, Lu X. Cortical control of motor sequences. Curr Opin Neurobiol. 2006; 16(2):213–21. [PubMed: 16563734]

Averbeck BB, Chafee MV, Crowe DA, Georgopoulos AP. Parallel processing of serial movements in prefrontal cortex. Proc Natl Acad Sci U S A. 2002; 99(20):13172–7. [PubMed: 12242330]

Averbeck BB, Chafee MV, Crowe DA, Georgopoulos AP. Neural activity in prefrontal cortex during copying geometrical shapes. I. Single cells encode shape, sequence, and metric parameters. Exp Brain Res. 2003; 150(2):127–41. [PubMed: 12669170]

Averbeck BB, Sohn JW, Lee D. Activity in prefrontal cortex during dynamic selection of action sequences. Nat Neurosci. 2006; 9(2):276–82. [PubMed: 16429134]

Cassim F, Monaca C, Szurhaj W, Bourriez JL, Defebvre L, Derambure P, Guieu JD. Does post-movement beta synchronization reflect an idling motor cortex? Neuroreport. 2001; 12(17):3859–63. [PubMed: 11726809]

Chan RC, Rao H, Chen EE, Ye B, Zhang C. The neural basis of motor sequencing: an fMRI study of healthy subjects. Neurosci Lett. 2006; 398(3):189–94. [PubMed: 16469446]

Chao CC, Karabanov AN, Paine R, Carolina de Campos A, Kukke SN, Wu T, Wang H, Hallett M. Induction of Motor Associative Plasticity in the Posterior Parietal Cortex-Primary Motor Network. Cereb Cortex. 2013

Cheyne D, Bakhtazad L, Gaetz W. Spatiotemporal mapping of cortical activity accompanying voluntary movements using an event-related beamforming approach. Hum Brain Mapp. 2006; 27(3):213–29. [PubMed: 16037985]

Cheyne D, Bells S, Ferrari P, Gaetz W, Bostan AC. Self-paced movements induce high-frequency gamma oscillations in primary motor cortex. Neuroimage. 2008; 42(1):332–42. [PubMed: 18511304]

Convento S, Bolognini N, Fusaro M, Lollo F, Vallar G. Neuromodulation of parietal and motor activity affects motor planning and execution. Cortex. 2014; 57:51–9. [PubMed: 24769545]

Cui H, Andersen RA. Different representations of potential and selected motor plans by distinct parietal areas. J Neurosci. 2011; 31(49):18130–6. [PubMed: 22159124]

Doyle LM, Yarrow K, Brown P. Lateralization of event-related beta desynchronization in the EEG during pre-cued reaction time tasks. Clin Neurophysiol. 2005; 116(8):1879–88. [PubMed: 15979401]

Engel AK, Fries P. Beta-band oscillations--signalling the status quo? Curr Opin Neurobiol. 2010; 20(2):156–65. [PubMed: 20359884]

Ernst MD. Permutation methods: A basis for exact inference. Stat Sci. 2004; 19:676–685.

Gaetz W, Cheyne D. Localization of sensorimotor cortical rhythms induced by tactile stimulation using spatially filtered MEG. Neuroimage. 2006; 30(3):899–908. [PubMed: 16326116]

Gaetz W, Edgar JC, Wang DJ, Roberts TP. Relating MEG measured motor cortical oscillations to resting gamma-aminobutyric acid (GABA) concentration. Neuroimage. 2011; 55(2):616–21. [PubMed: 21215806]

Gaetz W, Macdonald M, Cheyne D, Snead OC. Neuromagnetic imaging of movement-related cortical oscillations in children and adults: age predicts post-movement beta rebound. Neuroimage. 2010; 51(2):792–807. [PubMed: 20116434]

Glickstein M, Doron K. Cerebellum: connections and functions. Cerebellum. 2008; 7(4):589–94. [PubMed: 19002543]

Grent-'t-Jong T, Oostenveld R, Jensen O, Medendorp WP, Praamstra P. Competitive interactions in sensorimotor cortex: oscillations express separation between alternative movement targets. J Neurophysiol. 2014; 112(2):224–32. [PubMed: 24760786]

Gross J, Kujala J, Hamalainen M, Timmermann L, Schnitzler A, Salmelin R. Dynamic imaging of coherent sources: Studying neural interactions in the human brain. Proc Natl Acad Sci U S A. 2001; 98(2):694–9. [PubMed: 11209067]

Gross J, Pollok B, Dirks M, Timmermann L, Butz M, Schnitzler A. Task-dependent oscillations during unimanual and bimanual movements in the human primary motor cortex and SMA studied with magnetoencephalography. Neuroimage. 2005; 26(1):91–8. [PubMed: 15862209]

Hall SD, Stanford IM, Yamawaki N, McAllister CJ, Ronnqvist KC, Woodhall GL, Furlong PL. The role of GABAergic modulation in motor function related neuronal network activity. Neuroimage. 2011; 56(3):1506–10. [PubMed: 21320607]

Heinrichs-Graham E, Kurz MJ, Becker KM, Santamaria PM, Gendelman HE, Wilson TW. Hypersynchrony despite pathologically reduced beta oscillations in patients with Parkinson's disease: a pharmaco-magnetoencephalography study. J Neurophysiol. 2014a; 112(7):1739–47. [PubMed: 25008416]

Heinrichs-Graham E, Wilson TW, Santamaria PM, Heithoff SK, Torres-Russotto D, Hutter-Saunders JA, Estes KA, Meza JL, Mosley RL, Gendelman HE. Neuromagnetic evidence of abnormal movement-related beta desynchronization in Parkinson's disease. Cereb Cortex. 2014b; 24(10): 2669–78. [PubMed: 23645717]

Hoshi E, Tanji J. Differential roles of neuronal activity in the supplementary and presupplementary motor areas: from information retrieval to motor planning and execution. J Neurophysiol. 2004; 92(6):3482–99. [PubMed: 15269227]

Houdayer E, Labyt E, Cassim F, Bourriez JL, Derambure P. Relationship between event-related beta synchronization and afferent inputs: analysis of finger movement and peripheral nerve stimulations. Clin Neurophysiol. 2006; 117(3):628–36. [PubMed: 16427358]

Joundi RA, Jenkinson N, Brittain JS, Aziz TZ, Brown P. Driving oscillatory activity in the human cortex enhances motor performance. Curr Biol. 2012; 22(5):403–7. [PubMed: 22305755]

Jurkiewicz MT, Gaetz WC, Bostan AC, Cheyne D. Post-movement beta rebound is generated in motor cortex: evidence from neuromagnetic recordings. Neuroimage. 2006; 32(3):1281–9. [PubMed: 16863693]

Kaiser J, Birbaumer N, Lutzenberger W. Event-related beta desynchronization indicates timing of response selection in a delayed-response paradigm in humans. Neurosci Lett. 2001; 312(3):149–52. [PubMed: 11602332]

Krause V, Weber J, Pollok B. The Posterior Parietal Cortex (PPC) Mediates Anticipatory Motor Control. Brain Stimul. 2014

Kurz MJ, Becker KM, Heinrichs-Graham E, Wilson TW. Neurophysiological abnormalities in the sensorimotor cortices during the motor planning and movement execution stages of children with cerebral palsy. Dev Med Child Neurol. 2014; 56(11):1072–7. [PubMed: 24931008]

Lachaux JP, Rodriguez E, Martinerie J, Varela FJ. Measuring phase synchrony in brain signals. Hum Brain Mapp. 1999; 8(4):194–208. [PubMed: 10619414]

Maris E, Oostenveld R. Nonparametric statistical testing of EEG- and MEG-data. J Neurosci Methods. 2007; 164(1):177–90. [PubMed: 17517438]

Muthukumaraswamy SD. Functional properties of human primary motor cortex gamma oscillations. J Neurophysiol. 2010; 104(5):2873–85. [PubMed: 20884762]

Nachev P, Kennard C, Husain M. Functional role of the supplementary and pre-supplementary motor areas. Nat Rev Neurosci. 2008; 9(11):856–69. [PubMed: 18843271]

O'Neill GC, Bauer M, Woolrich MW, Morris PG, Barnes GR, Brookes MJ. Dynamic recruitment of resting state sub-networks. Neuroimage. 2015; 115:85–95. [PubMed: 25899137]

Papp N, Ktonas P. Critical evaluation of complex demodulation techniques for the quantification of bioelectrical activity. Biomed Sci Instrum. 1977; 13:135–45. [PubMed: 871500]

Park H, Kim JS, Chung CK. Differential beta-band event-related desynchronization during categorical action sequence planning. PLoS One. 2013; 8(3):e59544. [PubMed: 23527215]

Parkes LM, Bastiaansen MC, Norris DG. Combining EEG and fMRI to investigate the post-movement beta rebound. Neuroimage. 2006; 29(3):685–96. [PubMed: 16242346]

Pfurtscheller G, Lopes da Silva FH. Event-related EEG/MEG synchronization and desynchronization: basic principles. Clin Neurophysiol. 1999; 110(11):1842–57. [PubMed: 10576479]

Pfurtscheller G, Neuper C, Andrew C, Edlinger G. Foot and hand area mu rhythms. Int J Psychophysiol. 1997; 26(1-3):121–35. [PubMed: 9202999]

Pogosyan A, Gaynor LD, Eusebio A, Brown P. Boosting cortical activity at Beta-band frequencies slows movement in humans. Curr Biol. 2009; 19(19):1637–41. [PubMed: 19800236]

Pollok B, Gross J, Kamp D, Schnitzler A. Evidence for anticipatory motor control within a cerebello-diencephalic-parietal network. J Cogn Neurosci. 2008; 20(5):828–40. [PubMed: 18201129]

Pollok B, Gross J, Schnitzler A. How the brain controls repetitive finger movements. J Physiol Paris. 2006; 99(1):8–13. [PubMed: 16039102]

Pollok B, Krause V, Butz M, Schnitzler A. Modality specific functional interaction in sensorimotor synchronization. Hum Brain Mapp. 2009; 30(6):1783–90. [PubMed: 19301250]

Rocca MA, Gatti R, Agosta F, Broglia P, Rossi P, Riboldi E, Corti M, Comi G, Filippi M. Influence of task complexity during coordinated hand and foot movements in MS patients with and without fatigue. A kinematic and functional MRI study. J Neurol. 2009; 256(3):470–82. [PubMed: 19271107]

Salenius S, Schnitzler A, Salmelin R, Jousmaki V, Hari R. Modulation of human cortical rolandic rhythms during natural sensorimotor tasks. Neuroimage. 1997; 5(3):221–8. [PubMed: 9345551]

Schnitzler A, Salenius S, Salmelin R, Jousmaki V, Hari R. Involvement of primary motor cortex in motor imagery: a neuromagnetic study. Neuroimage. 1997; 6(3):201–8. [PubMed: 9344824]

Schoffelen JM, Oostenveld R, Fries P. Imaging the human motor system's beta-band synchronization during isometric contraction. Neuroimage. 2008; 41(2):437–47. [PubMed: 18396062]

Stefanescu MR, Thurling M, Maderwald S, Wiestler T, Ladd ME, Diedrichsen J, Timmann D. A 7T fMRI study of cerebellar activation in sequential finger movement tasks. Exp Brain Res. 2013; 228(2):243–54. [PubMed: 23732948]

Talairach, G.; Tournoux, P. −planar stereotaxic atlas of the human brain. Thieme; New York, NY: 1988.

Taulu S, Simola J. Spatiotemporal signal space separation method for rejecting nearby interference in MEG measurements. Phys Med Biol. 2006; 51(7):1759–68. [PubMed: 16552102]

Taulu S, Simola J, Kajola M. Applications of the signal space separation method (SSS). IEEE Trans Signal Process. 2005; 53(9):3359–3372.

Thoenissen D, Zilles K, Toni I. Differential involvement of parietal and precentral regions in movement preparation and motor intention. J Neurosci. 2002; 22(20):9024–34. [PubMed: 12388609]

Tzagarakis C, Ince NF, Leuthold AC, Pellizzer G. Beta-band activity during motor planning reflects response uncertainty. J Neurosci. 2010; 30(34):11270–7. [PubMed: 20739547]

Uusitalo MA, Ilmoniemi RJ. Signal-space projection method for separating MEG or EEG into components. Med Biol Eng Comput. 1997; 35(2):135–40. [PubMed: 9136207]

Van Veen BD, van Drongelen W, Yuchtman M, Suzuki A. Localization of brain electrical activity via linearly constrained minimum variance spatial filtering. IEEE Trans Biomed Eng. 1997; 44(9): 867–80. [PubMed: 9282479]

Wilson TW, Heinrichs-Graham E, Becker KM. Circadian modulation of motor-related beta oscillatory responses. Neuroimage. 2014a; 102P2:531–539. [PubMed: 25128712]

Wilson TW, Kurz MJ, Arpin DJ. Functional specialization within the supplementary motor area: a fNIRS study of bimanual coordination. Neuroimage. 2014b; 85:445–50. Pt 1. [PubMed: 23664948]

Wilson TW, Slason E, Asherin R, Kronberg E, Reite ML, Teale PD, Rojas DC. An extended motor network generates beta and gamma oscillatory perturbations during development. Brain Cogn. 2010; 73(2):75–84. [PubMed: 20418003]

Wilson TW, Slason E, Asherin R, Kronberg E, Teale PD, Reite ML, Rojas DC. Abnormal gamma and beta MEG activity during finger movements in early-onset psychosis. Dev Neuropsychol. 2011; 36(5):596–613. [PubMed: 21667363]

Wilson TW, Heinrichs-Graham E, Robertson KR, Sandkovsky U, O'Neill J, Knott NL, Fox HS, Swindells S. Functional brain abnormalities during finger-tapping in HIV-infected older adults: a magnetoencephalography study. J Neuroimmune Pharmacol. 2013; 8(4):965–74. [PubMed: 23749418]

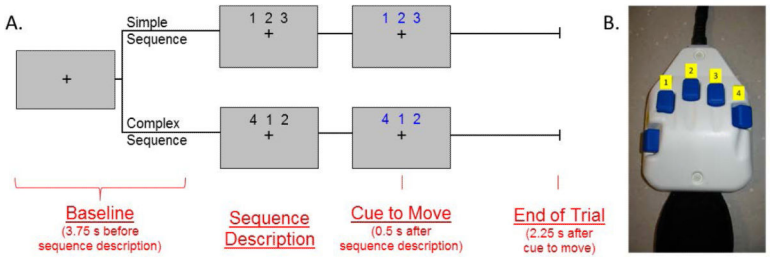

Figure 1. Task paradigm

A) Prior to the start of each trial, participants fixated on a crosshair for 3.75 s. After this baseline period, a series of three numbers (each corresponding to a digit on the finger) appeared on the screen for 0.5 s. There were two conditions corresponding to differing levels of motor plan complexity. In the "simple" condition, the series of numbers in the plan were sequential (i.e., "1-2-3", "2-3-4", "4-3-2" or "3-2-1"), and thus corresponded to tapping three adjacent fingers. In the "complex" condition, each number in the sequence was at least one number away from the previous number (i.e., "1-4-2", "2-4-1", "3-1-4", or "4-1-3"), and thus mapped to a sequence in which the finger being tapped was not adjacent to the previous finger tapped. After the numbers were displayed in black for 0.5 s, the numbers changed color which cued the participant to move. The participant then had 2.25 s to complete the motor plan and return to rest. After 2.25 s, the numbers disappeared and only the fixation crosshair remained. This combination of slides constituted one trial. Trials were pseudo-randomized and a total of 80 trials for each condition were completed (160 total trials), totaling about 16 minutes for the task. ***B)*** The button pad used during this task. Each button on the pad corresponded to a specific finger; the thumb was not used for task performance.

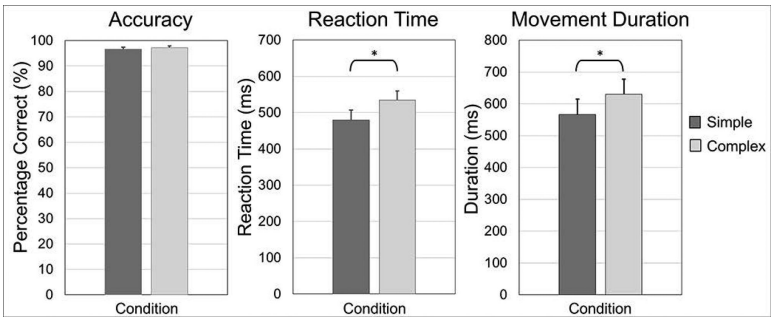

Figure 2. Behavioral results

In each bar graph, the simple condition is shown in dark gray, while the complex condition is shown in light gray. Error bars denote the standard error of the mean (SEM). Accuracy (percentage correct) is shown in the left panel. Participants performed generally well, and there was no significant difference in accuracy between the conditions, $t(16) = 0.940$, $p = 0.361$. Reaction time (in ms) is shown in the center panel. Participants had significantly slower reaction time in the complex compared to the simple condition, $t(16) = 5.45$, $p < .001$. The right panel shows mean movement durations for each condition. There was a significant increase in movement duration in the complex compared to the simple condition, $t(16) = 4.27$, $p < .001$. To control for these behavioral differences in the MEG analyses, we synced our MEG data with movement onset in each trial and focused all analyses on the time windows preceding and during the early stages of movement execution (i.e., before movement termination).

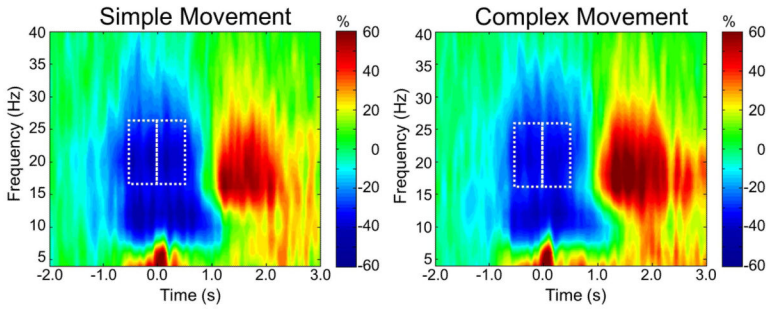

Figure 3. Group-averaged time-frequency spectra during simple and complex movements

Time (in s) is denoted on the x-axis, with 0.0 s defined as movement onset. Frequency (in Hz) is shown on the y-axis. All signal power data is expressed as a percent difference from baseline, with the color legend shown to the far right. Data represent a group-averaged gradiometer sensor near the left sensorimotor cortex (the same sensor was selected in each participant), and was computed separately for the simple (left panel) and complex movement (right panel) conditions. Prior to and during movement, there was a strong alpha/beta desynchronization (ERD) in both conditions. In many sensors, a break between alpha and beta ERD responses could be discerned, with clearly weaker activity between 12-15 Hz. After movement offset, participants exhibited a strong PMBR in both conditions. The white boxes in each image denote the time-frequency bins that were selected for beamforming analysis. The motor planning stage was imaged from −0.45 to 0.0 s at 16-26 Hz, whereas motor execution was imaged from 0.0 to 0.45 s at 16-26 Hz. The same time-frequency bins were imaged for both simple and complex movements.

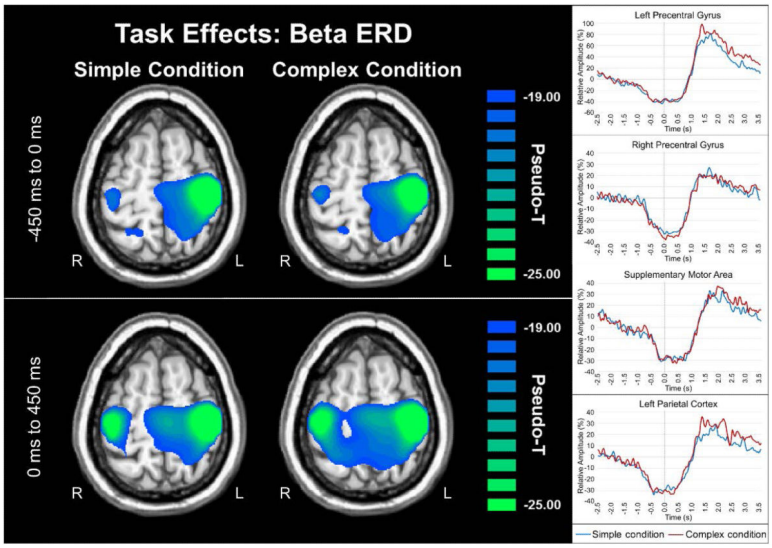

Figure 4. Beta ERD during movement planning and execution

Group mean beamformer images (pseudo-t) of beta activity during movement planning (top left) and execution (bottom left) time bins are shown with virtual sensor data to the right. During both simple and complex movements participants exhibited significant beta ERD task effects in the bilateral primary motor cortex (stronger in the contralateral), superior parietal regions, cerebellum (not shown) and the SMA during both time windows (all p's < . 0001, corrected). To more precisely examine the dynamics, virtual sensors from the peak voxel in each region were extracted (right panel), which further confirmed the temporal progression of neuronal activity that was discernable in the discrete beamformer images. For each voxel time series, relative amplitude (in percentage from baseline) is shown on the y-axis, with time (in seconds) on the x-axis. The simple condition is shown with a blue line, while the complex condition is shown in red. Axial slices are shown in radiologic convention (right = left).

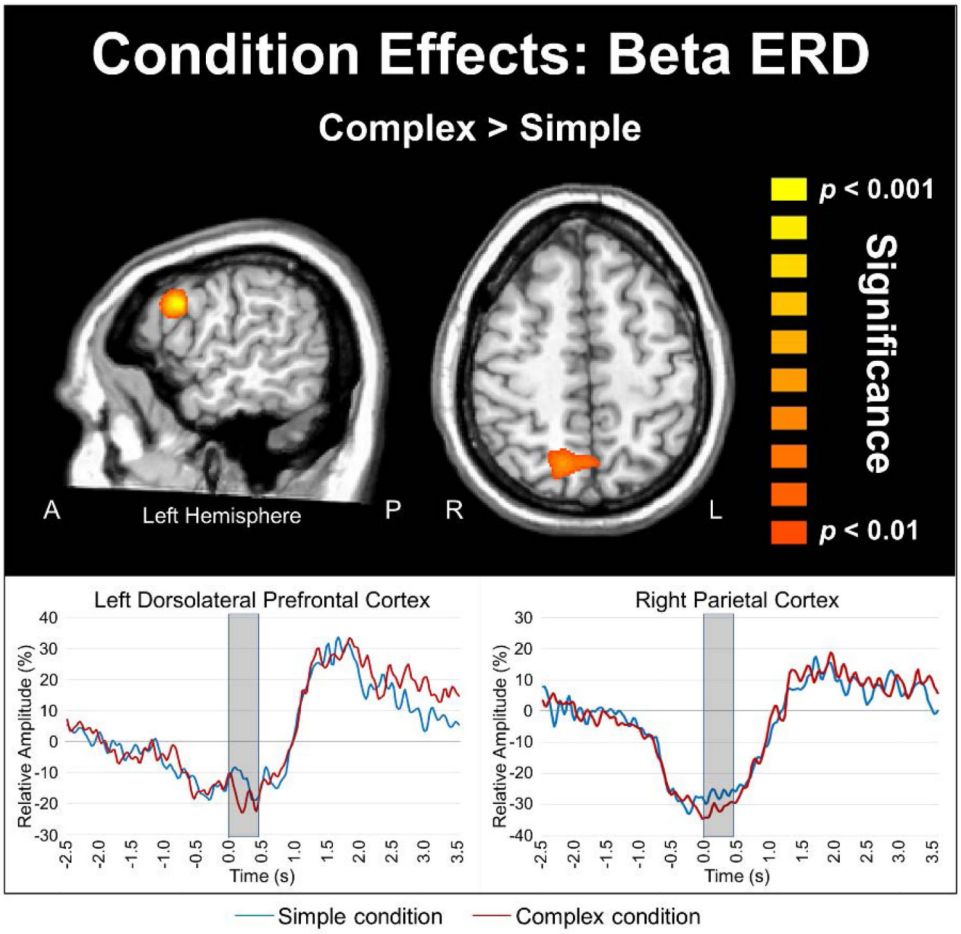

Figure 5. Stronger beta ERD amplitude during complex movements

Participants exhibited significantly stronger beta ERD in the left DLPFC ($p < .001$, corrected) and the right superior parietal cortices ($p < .001$, corrected) during the execution of complex relative to simple movements (0.0 to 0.45 s, 16-26 Hz). There were no significant differences ($p > .10$, corrected) between complex and simple sequences during the motor planning stage. For the time series, the simple condition is shown with a blue line, while the complex condition is shown in red. Axial slices are shown in radiologic convention (right = left).

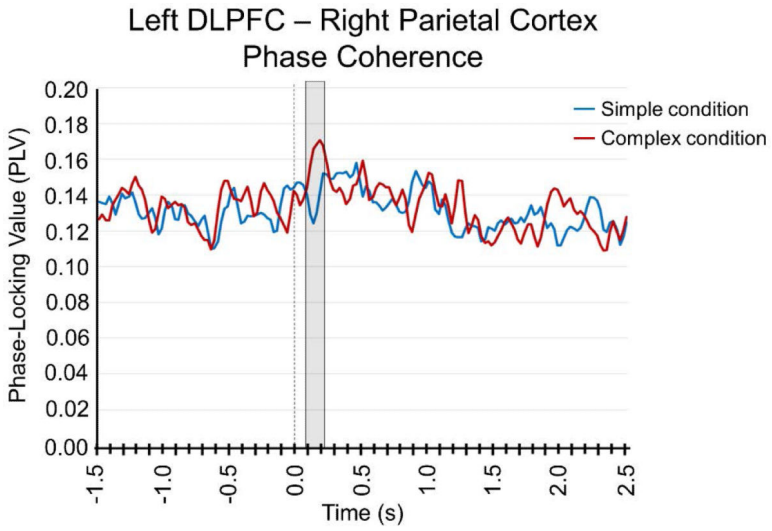

Figure 6. Phase coherence dynamics between the parietal and prefrontal cortices

There was a significant increase in beta phase synchrony between the right parietal cortices and the left DLPFC from 0.075 to 0.175 s after movement onset during the complex **(red line)** compared to the simple **(blue line)** condition ($p = 0.05$, corrected). Specifically, phase coherence (i.e., PLV) in the two conditions was relatively equal throughout the trial, but there was a sharp, transient increase in phase coherence shortly after movement onset (i.e., 0.075 to 0.175 s) in the complex condition that did not occur in the simple condition. The phase-locking value (PLV) is shown on the y-axis, while time (in seconds) is shown on the x-axis. In both panels, the shaded area denotes time bins where the two conditions (i.e., complex and simple) significantly differed.